# Multiscale Force Networks in Highly Polydisperse Granular Media

C. Voivret, F. Radjaï, J.-Y. Delenne, and M. S. El Youssoufi

*LMGC, CNRS-Université Montpellier 2, Place Eugène Bataillon, 34095 Montpellier cedex, France*

(Received 26 January 2009; published 29 April 2009)

We investigate highly polydisperse packings subjected to simple shear by contact dynamics simulations. A major unsolved issue is how granular texture and force chains depend on the size polydispersity and how far they influence the shear strength. The numerical treatment was made possible by ensuring the statistical representativity of particle size classes. An unexpected finding is that the internal friction angle is independent of polydispersity. We show that this behavior is related to two mechanisms underlying the stability of force chains: (i) The class of largest particles captures strong force chains, and (ii) these chains are equilibrated by weak forces carried by increasingly smaller particles as the size span broadens. In the presence of adhesion between particles, the Coulomb cohesion increases with size polydispersity as a result of enhanced force anisotropy.

DOI: 10.1103/PhysRevLett.102.178001 PACS numbers: 45.70.−n, 61.43.−j, 81.05.Rm

Most granular materials occurring in nature and industrial application are composed of a broad range of particle sizes [1,2]. Size polydispersity is a key to the space-filling and strength properties of granular materials, and for this reason it needs to be optimized in designing particle-based materials such as concrete [3–5]. However, most research work has focused on model granular systems composed of nearly monosized particles. In highly polydisperse granular materials, the particles of a given size can fit into the pores between larger particles. Hence, the space is filled in a hierarchical manner as in Apollonian packings [3]. However, unlike Apollonian packings in which the fine adjustment of particle positions leads to a fractal structure, the polydisperse granular media are generically disordered, and their multiscale microstructure is a consequence of the filling procedure. Novel features are thus expected to emerge due to force transmission through a disordered contact network involving a hierarchy of length scales.

The difficulty for a systematic investigation lies mainly in the preparation of well-calibrated polydisperse samples of the same material in order to be able to isolate properly the effect of polydispersity from other factors such as particle shape, surface effect, etc. On the other hand, a few existing theoretical models have been essentially concerned with a solid fraction constructed according to particular space-filling strategies [2,6–8].

In this Letter, we use numerical simulations to investigate the shear behavior and force transmission in highly polydisperse granular media. We developed a numerical approach allowing us to prepare and shear large packings of circular particles of variable size distribution. The challenge is that a broad size distribution with well-represented populations of different sizes requires many more particles than a narrow distribution [9]. In the following, we briefly describe our approach that combines three ingredients: (i) a generic size distribution function, (ii) an efficient assembling method, and (iii) a fast dynamic method for shearing the granular samples.

The size distribution is represented by the cumulate volume distribution defined as the cumulative volume $h(d)$ of the particles as a function of particle diameter $d$. We use a distribution function based on the cumulative $\beta$ distribution which allows us to generate a broad range of distributions with only two parameters controlling the shape of the distribution. The size span is defined by $s = (d_{\max} - d_{\min})/(d_{\max} + d_{\min})$, where $d_{\min}$ and $d_{\max}$ are the smallest and largest diameters, respectively. A monodisperse distribution corresponds to $s = 0$, and the limit $s \simeq 1$ corresponds to an infinitely polydisperse system [9].

For assembling the particles into a dense packing, we use a geometrical deposition method according to simple geometrical rules [10]. Each particle is deposited over those already deposited in the lowest position at the free surface. This method is efficiently implemented in a computer code with periodic boundary conditions in the horizontal direction. The packings prepared by this method are homogeneous in particle size and thus involve no size segregation.

The packings prepared by geometrical procedure are allowed to relax to static equilibrium under a constant vertical stress $\sigma_v$ applied on the upper wall. The gravity is set to zero in order to avoid stress gradients. The simulations are performed by means of the contact dynamics method [11,12], which is the genuine method for the simulation of perfectly rigid particles. We simulated several packings of $10^4$ particles with the size span $s$ varying from $s = 0.2$ to $s = 0.96$. During relaxation, the coefficient of friction between particles is set to zero in order to obtain nearly isotropic and dense packings. At the end of relaxation, the solid fraction $\rho$ for each value of $s$ is slightly above its value in the geometrically deposited packing. It varies nonlinearly from $\rho = 0.82$ for $s = 0.2$ to $\rho = 0.92$ for $s = 0.96$. Two conditions are required to fill efficiently the pores: (i) a broad size distribution, which corresponds to higher values of $s$ ($s > 0.4$ in our simulations), and (ii) a large number of smaller particles, controlled in our model

 

by the shape parameters. A parametric study of the solid fraction as a function of shape parameters shows that the largest value of the solid fraction is obtained with a uniform distribution by particle volume fraction defined by $h(d) = (d - d_{\min})/(d_{\max} - d_{\min})$. The above condition appears therefore to be best met for this distribution. The results presented below were obtained with this distribution, although they remain valid irrespective of shape parameters. Given the disordered microstructure of these samples with an optimal filling of space, they can be qualified as polydisperse random close packings.

The coefficient of friction between particles is set to $\mu = 0.4$ in the relaxed packings, and they are sheared by subjecting the upper wall to a small horizontal velocity $v$ and constant confining pressure $\sigma_v$ while the lower wall is kept immobile. During shear, all samples dilate from their initially high density and tend to a constant solid fraction in the steady state depending on $s$. The stress tensor in the sample is given by $\sigma_{ij} = n_c \langle f_i^c \ell_j^c \rangle$, where $n_c$ is the number density of contact and the average is taken over the contacts $c$ with contact force $f^c$ and branch vector $\ell^c$ joining the centers of contacting particles [13–16]. The mean stress is $p = (\sigma_1 + \sigma_2)/2$, where $\sigma_1$ and $\sigma_2$ are the principal stress values. We also define a stress deviator $q = (\sigma_1 - \sigma_2)/2$. During shear, the shear stress jumps initially to a high value before decreasing to a nearly constant value in the steady state. The steady-state shear stress $q^*/p$ characterizes the shear strength of the material. According to the Mohr-Coulomb model, the shear strength of granular materials can be split in two contributions: (i) the internal angle of friction $\varphi$ and (ii) the Coulomb cohesion $c$. In 2D, these two parameters are related to $q^*$ by [1]

$$q^* = p \sin\varphi^* + c \cos\varphi^*. \tag{1}$$

Figure 1 shows $\varphi^*$ as a function of $s$ for cohesionless packings. Surprisingly, we observe that $\varphi^*$ is almost independent of size span $s$. This result is rather counterintuitive as it is often believed that the shear strength in granular materials should increase with the solid fraction, which is an increasing function of $s$. In order to understand the origin of this paradox, we analyzed in the following the microstructure and force transmission.

Figure 2 displays a snapshot of the force network for $s = 0.96$. We observe strong force chains preferentially passing through larger particles. At the same time, a large number of small particles are excluded from the force network. In other words, the large particles capture the strongest force chains, whereas small particles often miss them. The packing becomes therefore more inhomogeneous in force transmission as the size span becomes broader. This is best illustrated by the probability density function (PDF) of normal forces shown in Fig. 3 for different values of $s$ [13]. We see that the PDF becomes broader as $s$ increases, and it takes a decreasing power-law form ($\propto f^{-\alpha}$) in the range of weak forces (below the mean force) with an increasing exponent as a function of $s$. This enhanced force inhomogeneity is in strong contrast with the fact that the packing becomes more homogeneous in terms of the solid fraction as the size span broadens.

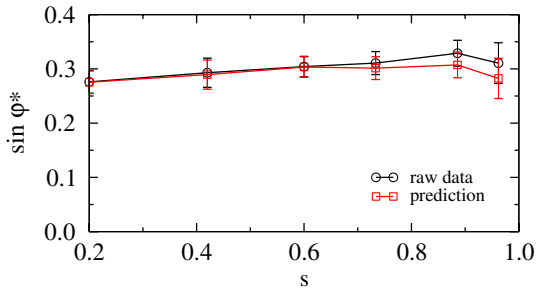


FIG. 1 (color online). Internal friction $\sin\varphi^*$ as a function of particle size span $s$ both from raw simulation data and as predicted by Eq. (5). The error bars indicate the standard deviation of stress fluctuations in the steady state.

The force network is linked with the stress components via the expression of the stress tensor that we write down here in its integral form [13–16]:

$$\sigma_{\alpha\beta} = n_c \iiint f_\alpha(\vec{n}) \ell_\beta(\vec{n}) P_{f\ell n}(\vec{f}, \ell, \vec{n}) d\vec{f} d\ell d\vec{n}, \tag{2}$$

where $P_{f\ell n}(\vec{f}, \ell, \vec{n})$ is the joint PDF of the forces $\vec{f}$ and branch vectors $\vec{\ell} = \ell\vec{n}$ . At the lowest-order description of the force network, we neglect the correlations and split the joint probability function as a product of three independent functions $P_{f\ell n}(\vec{f}, \ell, \vec{n}) = P_f(\vec{f}) P_\ell(\ell) P_n(\vec{n})$. Then integration over $\vec{f}$ and $\ell$ yields

$$\sigma_{\alpha\beta} \simeq n_c \int_\Omega \langle f_\alpha \rangle(\vec{n}) \langle \ell_\beta \rangle(\vec{n}) P_n(\vec{n}) d\vec{n}, \tag{3}$$

where $\Omega$ is the angular domain of integration and $\langle \ell \rangle(\vec{n})$ and $\langle f \rangle(\vec{n})$ are the average branch vector length and force as a function of contact orientation vector $\vec{n} \equiv (\cos\theta, \sin\theta)$ in 2D, respectively. In this framework, a model of stress transmission is reduced to the choice of the functions $\langle \ell \rangle \times (\theta)$, $\langle \vec{f} \rangle(\theta)$, and $P_n(\theta)$. The contact force $\vec{f}$ can be represented by its normal and tangential components $f_n(\theta)$ and $f_t(\theta)$, respectively.

The above four functions describe the general state of the packing. Under shearing, the packing self-organizes itself into a "pure" state where the state functions are well approximated by their lowest-order Fourier expansion [16,17]:

$$\begin{aligned} P_n(\theta) &\simeq \frac{1}{\pi}\{1 + a_c \cos 2(\theta - \theta_c)\}, \\ \langle \ell \rangle(\theta) &\simeq \langle \ell \rangle\{1 + a_\ell \cos 2(\theta - \theta_\ell)\}, \\ \langle f_n \rangle(\theta) &\simeq \langle f_n \rangle\{1 + a_n \cos 2(\theta - \theta_n)\}, \\ \langle f_t \rangle(\theta) &\simeq -\langle f_n \rangle a_t \sin 2(\theta - \theta_t), \end{aligned} \tag{4}$$

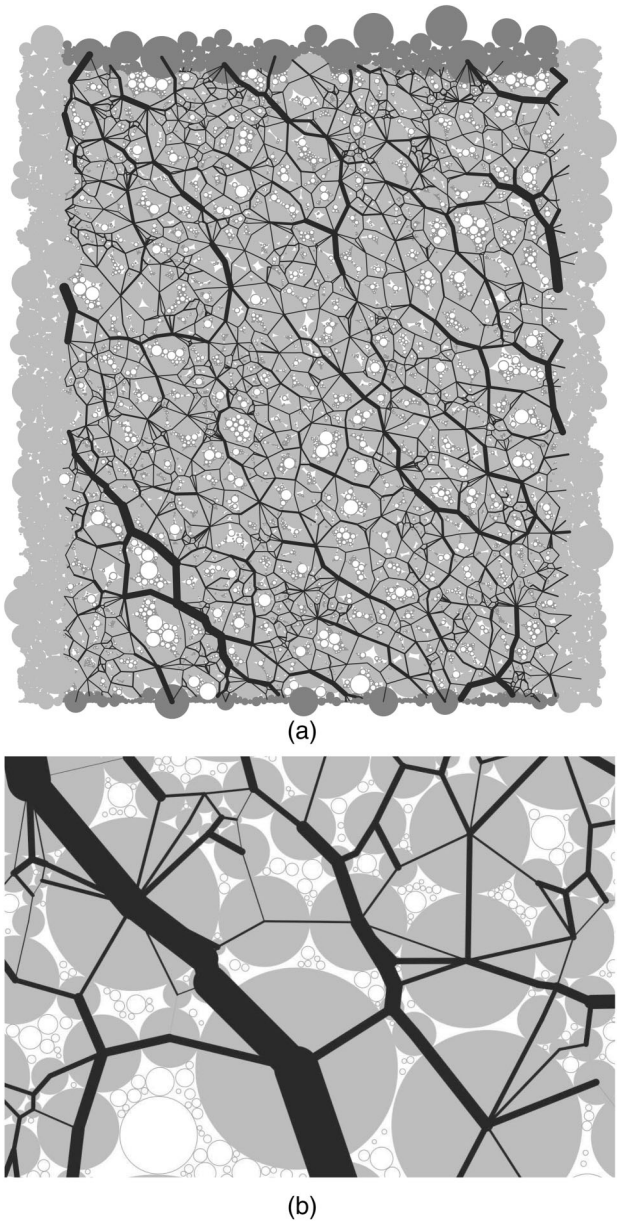


FIG. 2. A snapshot of a highly polydisperse packing with size span $s = 0.96$: (a) the entire sample and (b) a zoom. The floating particles excluded from the force network are in white. Line thickness is proportional to normal force.

where $a_c$, $a_\ell$, $a_n$, and $a_t$ are anisotropy parameters and the angles $\theta_c$, $\theta_\ell$, $\theta_n$, and $\theta_t$ represent the corresponding privileged directions; see Fig. 4. In general, the privileged angles can be all different, but in a sheared state they tend to follow the principal stress direction ($\theta_\sigma = \theta_c = \theta_\ell = \theta_n = \theta_t$). Now, inserting the Fourier expansions (4) into the integral expression (3) of stress and neglecting cross products between anisotropy parameters, one gets

$$\sin\varphi^* = \frac{q^*}{p} \simeq \frac{1}{2}(a_c + a_\ell + a_n + a_t). \tag{5}$$

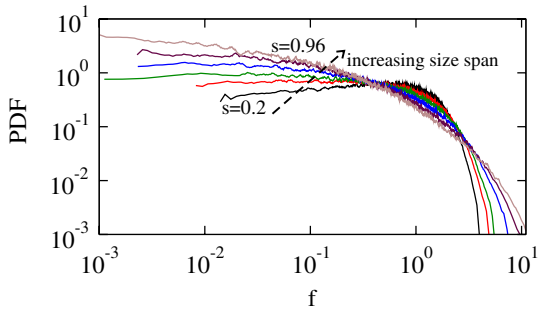


FIG. 3 (color online). Probability distribution function of normal forces $f = f_n/\langle f_n\rangle$ normalized by the average force $\langle f_n\rangle$ for different values of size span $s$.

The predicted values of $\sin\varphi^*$ by this equation are shown in Fig. 1 together with the measured values as a function of $s$. We see that Eq. (5) approximates well the friction angle for all values of $s$.

The evolution of the four anisotropies with $s$ is displayed in Fig. 4 from the simulation data. Interestingly, the force anisotropies $a_n$ and $a_t$ are independent of $s$. This is consistent with the observation that the strong force chains, underlying the force anisotropies for the most part, are mainly guided by the class of largest particles irrespective of $s$. However, the contact orientation anisotropy $a_c$ declines with $s$, reflecting the fact that the larger particles are surrounded by an increasing number of small particles as $s$ increases. At the same time, the length anisotropy $a_\ell$ increases with $s$ since the longest branch vectors occur between the largest particles that align themselves with the strong force chains. It is remarkable that $a_c$ and $a_\ell$ evolve with $s$ but their sum $a_c + a_\ell$ remains constant. By virtue of Eq. (5), this compensation between $a_c$ and $a_l$, together with the fact that $a_n$ and $a_t$ do not evolve with $s$, implies that $\varphi^*$ is independent of the size span. In this way, the independence of the internal friction angle with respect to size polydispersity appears to be a consequence of the multi-

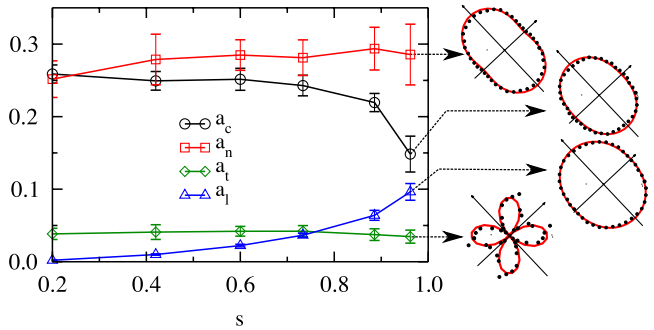


FIG. 4 (color online). Evolution of state anisotropies as a function of the size span in the steady shear state. The error bars correspond to the standard deviation of the fluctuations in the steady state. The polar diagrams of the corresponding angular distributions (black symbols) are shown for $s = 0.96$ together with their fits (red) by truncated Fourier expansions [Eq. (4)].

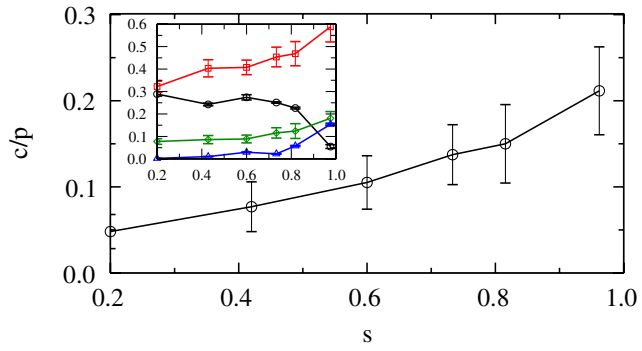


FIG. 5 (color online). Evolution of Coulomb cohesion $c$ normalized by the average pressure in the steady state as a function of size span $s$. The error bars correspond to the standard deviation of stress fluctuations in the steady state. The inset shows the steady-state anisotropies as a function of $s$.

scale nature of the force network. Schematically, the force chains cascade from large scales (large particles) down to small scales (small particles), and the effect of increasing the size span is to replace the particles propping the strong force chains by a growing population of smaller particles.

In order to elucidate the effect of polydispersity in the presence of cohesion, we performed simple shear simulations under the same boundary conditions as before but with an additional constant adhesion force $-f_0$ between contacting particles. The adhesion force being reversible, we obtain cohesive packings with well-defined shear strength in the steady state. We find that the shear strength $q^*/p$ increases with $s$, whereas $\varphi^*$ keeps the same value as in cohesionless packings. Hence, according to Eq. (1), the Coulomb cohesion $c$ increases with size span $s$ as shown in Fig. 5. We see that the main contribution to cohesion stems from the force anisotropies $a_n$ and $a_t$ that increase with $s$ given the same constant value of local adhesion. In other words, the effect of adhesion is enhanced by size polydispersity.

In summary, our simulations provide clear evidence that, in highly polydisperse granular media, the internal friction angle is independent with respect to the particle size span. This unexpected feature was shown to be a consequence of the interplay between force chains and a hierarchy of length scales. Our results also clarify the amplifying effect of polydispersity on the Coulomb cohesion of cohesive granular materials.

Our findings are relevant to a wide class of granular materials where size polydispersity and adhesion are essential to the behavior. Since the force networks present generally similar phenomenology in 2D and 3D, we expect that our results will apply also in 3D. Presently, 3D simulations are under way but require considerably more particles for the sake of statistical representativity of size populations and thus much more demanding computation time.

[1] J. K. Mitchell and K. Soga, *Fundamentals of Soil Behavior* (Wiley, New York, 2005), 3rd ed.
[2] T. Aste and D. Weaire, *The Pursuit of Perfect Packing* (Institute of Physics Publishing, Bristol, 2000).
[3] H. J. Herrmann, R. Mahmoodi Baram, and M. Wackenhut, Physica (Amsterdam) **330A**, 77 (2003).
[4] F. de Larrard, *Concrete Mixture Proportioning* (E & FN Spon, London, 1999).
[5] H. J. Herrmann, J. A. Astrom, and R. Mahmoodi Baram, Physica (Amsterdam) **344A**, 516 (2004).
[6] A. Gervois, C. Annic, J. Lemaitre, M. Ammi, L. Oger, and J. P. Troadec, Physica (Amsterdam) **218A**, 403 (1995).
[7] A. Gervois and D. Bideau, in *Disorder and Granular Media*, edited by D. Bideau (Elsevier, Amsterdam, 1993).
[8] P. Richard, L. Oger, J.-P. Troadec, and A. Gervois, Phys. Rev. E **60**, 4551 (1999).
[9] C. Voivret, F. Radjai, J.-Y. Delenne, and M. S. El Youssoufi, Phys. Rev. E **76**, 021301 (2007).
[10] W. M. Visscher and M. Bolstreli, Nature (London) **239**, 504 (1972).
[11] J. Moreau, Eur. J. Mech. A. Solids **13**, 93 (1994).
[12] F. Radjai, Eur. J. Environ. Civil Eng. **12**, 871 (2008).
[13] F. Radjai, D. E. Wolf, M. Jean, and J.-J. Moreau, Phys. Rev. Lett. **80**, 61 (1998).
[14] M. M. Mehrabadi, S. Nemat-Nasser, and M. Oda, Int. J. Numer. Anal. Meth. Geomech. **6**, 95 (1982).
[15] J. Christoffersen, M. M. Mehrabadi, and S. Nemat-Nasser, J. Appl. Mech. **48**, 339 (1981).
[16] L. Rothenburg and R. J. Bathurst, Geotechnique **39**, 601 (1989).
[17] B. Cambou, in *Proceedings of Powders and Grains 93*, edited by C. Thornton (A. A. Balkema, Amsterdam, 1993), pp. 73–86.